# Kinetics of in vitro digestion of starches monitored by time-resolved1H nuclear magnetic resonance

Anthony C. Dona, Guilhem Pages, Robert G. Gilbert, Marianne Gaborieau,
Philip W. Kuchel

# Kinetics of In Vitro Digestion of Starches Monitored by Time-Resolved H Nuclear Magnetic Resonance

Anthony C. Dona, Guilhem Pages, Robert G. Gilbert, Marianne Gaborieau, and Philip W. Kuchel

## More About This Article

Additional resources and features associated with this article are available within the HTML version:

- Supporting Information
- Access to high resolution figures
- Links to articles and content related to this article
- Copyright permission to reproduce figures and/or text from this article

View the Full Text HTML

# Kinetics of In Vitro Digestion of Starches Monitored by Time-Resolved $^1$H Nuclear Magnetic Resonance

Anthony C. Dona,[†,‡] Guilhem Pages,[†] Robert G. Gilbert,[‡] Marianne Gaborieau,[‡] and Philip W. Kuchel[*,†]

*School of Molecular and Microbial Biosciences, University of Sydney, Sydney, NSW 2006, Australia, and Centre for Nutrition and Food Sciences, Hartley Teakle Building 83, The University of Queensland, Brisbane QLD 4072, Australia*

A $^1$H NMR method is presented that monitors the initial and later stages of in vitro enzymatic digestion of starch suspensions. It allows, for the first time to our knowledge, the accurate analysis of the initial 5% of the extent of hydrolysis. This is significant because rapidly digested starch produces glucose that determines the blood glucose concentration immediately after ingestion of food. The two key hydrolytic enzymes, α-amylase and amyloglucosidase, showed clear systematic deviation from Michaelis–Menten kinetics as the starch or wheat flour substrate that was used changed its character during the reaction. Estimates of Michaelis–Menten parameters for amyloglucosidase and α-amylase were successfully found by analyzing two stages of digestion separately. The Michaelis–Menten constants for purified starch were $(6.4 \pm 0.8)$ and $(1.1 \pm 0.3)$ g $dL^{-1}$ (% w/v), respectively; and the maximum velocities of glucose release by amyloglucosidase, and short oligoglucosides and glucose by α-amylase were $(1.9 \pm 0.4) \times 10^{-2}$ and $(1.6 \pm 0.2) \times 10^{-2}$ mmol $L^{-1}$ $s^{-1}$ for the first stage of digestion, and $(9.0 \pm 1.0) \times 10^{-3}$ and $(4.7 \pm 1.4) \times 10^{-3}$ mmol $L^{-1}$ $s^{-1}$ for the second stage, giving a ratio of the two $V_{max}$ values of 2.1 and 3.4, respectively.

## Introduction

Starch comprises at least 50% of the food energy in most human and animal diets,[1,2] and given the growing incidence of nutrition-related diseases such as diabetes and obesity, it is important to develop techniques for monitoring the initial stages of digestion of starch-containing substrates. Starch in grains has an extremely complex structure, with up to six well identified different structural levels.[3,4] Differences in structure, on both molecular and supramolecular levels, give each starch species, and indeed each starch-containing food, unique characteristics of digestibility. However, it also makes starch difficult to characterize, leaving it far from completely understood as a macronutrient.[3]

Regardless of their botanical origins, starch varieties primarily contain two different types of dehydroglucose polymers, both connected by α-(1,4) linkages in linear segments and α-(1,6) linkages at branch points. Amylose consists largely of linear molecules with a few long branches;[5] amylopectin has many short branches with a nonrandom distribution[6] of branch points (4−5%) and is characteristically larger than amylose. Starch and starch-based foods have been characterized to some extent by nuclear magnetic resonance (NMR) spectroscopy.[7,8] The technique's versatility in analyzing complex biological samples[9−11] allows the investigation of characteristics of starch such as its molecular and supramolecular structure, molecular dynamics, dissolution kinetics, and water interactions.[12−15]

Many factors affect the digestibility of starch-containing foods, including the nature of the starch, the cooking method, and the presence of fiber, fat, and protein. Moreover, many intrinsic and extrinsic factors, including crystallinity, branching structure, weight distribution, and solubility, affect the nature of the starch and so affect its digestibility.[16,17] The digestibility of starch samples is currently measured by various different protocols, both in vivo[7,18,19] and in vitro.[20−23] A popular although controversial[24] index that expresses the relative rates of bioavailability of glucose from a food after its consumption is its glycemic index (GI).[25,26] The immediate effect of carbohydrates on an individual's blood glucose concentration is of interest not only for dietary design, but it also has implications for the obesity epidemic and it is functionally important in characterizing diets for the management of diabetes.[18,27]

The process of starch digestion in humans begins with α-amylase in the saliva (ptyalin) followed by pancreatic α-amylase; these are endohydrolases that cleave α-(1,4) linkages at random locations in the starch, creating maltose, oligoglucosides, α-dextrins, and small amounts of free glucose. Substances indigestible by α-amylase are converted into single glucose units. The conversion to glucose occurs by the action of enzymes incorporated in the plasma membrane of the small intestine including mucosal amyloglucosidase and sucrase-isomaltase. These enzymes are exoglucosidases acting on the nonreducing end of glucose oligomers catalyzing not only the hydrolysis of α-(1,4) linkages but also to a lesser extent α-(1,6) branch linkages, enabling the further degradation of nonlinear oligosaccharides.

Starch digestion has been divided into three categories for in vitro analysis:[19] rapidly digestible starch (RDS, digested in the first 20 min), slowly digestible starch (SDS, digested from 20 to 120 min), and resistant starch (RS, >120 min) using standardized concentrations of glucohydrolases. Techniques such as in vitro glucose assaying[22,28,29] and high-resolution magic-angle spinning (HR-MAS) $^1$H NMR[30] have been used in an effort to monitor glucose and oligoglucoside production;

**Table 1.** $T_1$ and $T_2$ Relaxation Times for the Various Carbohydrates

| water | $T_1$ relaxation (s) | | | $T_2$ relaxation (s) | | |
|---|---|---|---|---|---|---|
| | $0.10 \pm 0.02^a$ | | | $0.11 \pm 0.02$ | | |
| | $\alpha$-(1,4)-C$_1$H | $\beta$-(1,4)-C$_1$H | $\alpha$-(1,4) link-C$_1$H | $\alpha$-(1,4)-C$_1$H | $\beta$-(1,4)-C$_1$H | $\alpha$-(1,4) link-C$_1$H |
| glucose | $3.10 \pm 0.12$ | $1.78 \pm 0.07$ | N/A | $2.25 \pm 0.10$ | $0.28 \pm 0.05$ | N/A |
| maltotetraose | $2.20 \pm 0.09$ | $1.45 \pm 0.05$ | $1.13 \pm 0.05$ | $1.99 \pm 0.12$ | $0.5 \pm 0.07$ | $0.99 \pm 0.09$ |
| starch | $2.30 \pm 0.15$ | | $1.30 \pm 0.18$ | $1.07 \pm 0.12$ | | $0.41 \pm 0.12$ |

$^a$ Denotes $\pm$ standard deviation.

**Scheme 1.** Digestion of Starch by $\alpha$-Amylase and Amyloglucosidase
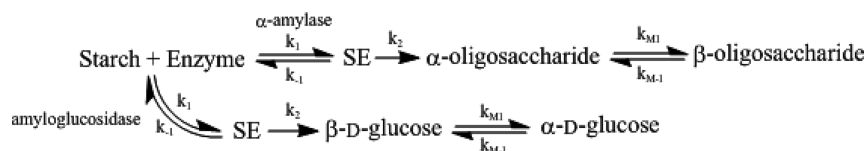


however, the important initial stages of digestion have been overlooked due to a lack of sensitivity with methods used for the low concentrations of glucose produced in this phase of the reaction, or due to an inability to collect data immediately after sample preparation.

Studies that have recorded the time courses[21,31−34] for the digestion of starch display stages that are separated by a discontinuity in the smoothness of the kinetic curves of sugar production. Furthermore, the amount of time taken for the RDS to be digested can vary depending on the conditions of digestion and will not always occur in the first 20 min.[31−34] Although multiple stages are obvious during starch digestion, attempts at characterizing the kinetics of starch hydrolysis have not considered two or more stages.[31,33,34]

The aim of this article is to introduce a new $^1$H solution-state NMR methodology for directly monitoring the $\alpha$- and $\beta$-reducing ends of oligoglucosides produced by enzymatic hydrolysis of starch and to present a different approach based on two or multiple steps to kinetically analyze the digestion of the carbohydrate. It enables accurate monitoring of the kinetics of the initial and later stages of starch hydrolysis over short time intervals using classical Michaelis−Menten kinetics. As the appearance of both $\alpha$- and $\beta$-anomers of glucose (or oligoglucosides) was monitored, it was also necessary to consider the kinetics of mutarotation between $\alpha$- and $\beta$-glucose and the oligoglucosides.

## Experimental Section

**Materials.** Rice starch was obtained from Sigma (S-7260; St Louis, MO) and the flour used was from wheat grown in 2005 at Griffith, NSW, Australia (Chara, Row 10, Plot 6:181). The enzymes were amyloglucosidase from *Aspergillus niger* (Sigma, A7095) used at a concentration of 300 U mL$^{-1}$, and $\alpha$-amylase (Megazyme; Wicklow, Ireland) used at a concentration of 3000 U mL$^{-1}$, where a single unit of enzyme hydrolyses 1 $\mu$mol min$^{-1}$ of $\alpha$-(1,4) linkage. Mutarotation kinetics and concentration-calibration experiments were carried out using anhydrous $\alpha$-D-glucose (AF404308; Ajax Finechems, NSW, Australia) and D-maltose monohydrate (Sigma, M5885) for verification.

**Methods.** *$^1$H Solution-State NMR Spectroscopy.* All NMR spectra were acquired on a Bruker DRX-400 spectrometer (Karlsruhe, Germany), equipped with a 9.4 T wide-bore vertical magnet (Oxford Instruments, Oxford, U.K.), operating at a radio frequency (RF) of 400.13 MHz for $^1$H detection, using a 5 mm triple resonance inverse (TXI) probe. The probe temperature was set to 25 °C for all experiments. Concentrations of starch solutions ranged from 0.5 to 6.0 g dL$^{-1}$ (% w/v). A Carr−Purcell−Meiboom−Gill (CPMG) pulse sequence was used with an echo time of 0.5 ms and an echo pulse train

of 100 repetitions;[35] it decreased the broadness of the solvent peak, as water has a short transverse relaxation time ($T_2$ Table 1), and was coupled with a water presaturation pulse (power attenuation, 55 dB) during the relaxation delay. Longitudinal relaxation time ($T_1$) and $T_2$ values for appropriate signals from relevant carbohydrates were measured by an inverse recovery and a CPMG pulse sequence, respectively (Table 1). The 90° pulse duration was around 11.5 $\mu$s; and the acquisition time (AQ) and relaxation delay ($d_1$) were 8 and 2 s, respectively. Each spectrum was derived from eight transients preceded by four dummy transients. The sample-spinning rate during the kinetic experiments was 20 Hz keeping the sample homogeneous in the vertical direction by avoiding sedimentation of the substrate. This also ensured that during the digestion solubilized starch substrate, product and solvent were in the receiver coil and moving sufficiently fast to give a resolved signal circumventing the need for consideration of mass transport of the solutes within the sample. The chemical shift was calibrated using signal from sodium 3-(trimethylsilyl)propane-1-sulfonate (DSS) signal at 0.000 ppm. The exponential line broadening used was 1 Hz and no zero-filling was applied. The data were recorded with XWINNMR 3.2 (Bruker) and processed using TOPSPIN 1.3 (Bruker).

To calibrate concentrations of $\alpha$- and $\beta$-reducing ends using the -C$_1$H resonance of glucose and oligoglucosides produced during hydrolysis, $^1$H NMR spectra of D-glucose standards were recorded (at five concentrations from 10 to 100 mmol L$^{-1}$) prior to each set of experiments. The D-glucose standards were tested against other oligosaccharides of the same concentration, which all exhibited insignificant differences of total signal from the reducing ends. The $T_1$ and $T_2$ relaxation times were measured for relevant signals in glucose and maltotetraose (Table 1), revealing little difference in this value between oligosaccharides of various lengths, validating any effects of the presaturation or cross relaxation did not affect the quantification of the analysis method. All digestions were carried out in 40 mmol L$^{-1}$ sodium acetate buffer, at pH 5.3 made up in D$_2$O, containing 10 mmol L$^{-1}$ DSS, internal standard for the quantification of the concentration of reducing-end glucoses. Prior to enzyme addition, a spectrum of each starch/flour suspension was obtained, and the integral of -C$_1$H resonance of the $\alpha$- and $\beta$-reducing ends was subtracted from the signal recorded during the time course. Enzyme solution (3 U mL$^{-1}$ for starch, 30 U mL$^{-1}$ for wheat flour) was added to the samples of different starch/flour concentrations [∼0.8, 1.5, 3, 4.5, 6 g dL$^{-1}$]. Between 40 and 60 $^1$H NMR spectra (∼2 min each) were acquired sequentially, immediately following the addition of enzyme, at 25 °C. The delay between beginning the enzymatic reaction and recording a $^1$H NMR spectrum was then precisely timed (∼2 min).

*Fitting Kinetic Data.* If the initial concentration of $\alpha$-glucose or $\alpha$-diglucoside (maltose) is $A_0$, then the rate of conversion between the anomers obeys the differential rate law[36]

$$\frac{d[\beta]}{dt} = k_{M1}(A_0 - [\beta]) - k_{M-1}[\beta] \tag{1}$$

where $[\beta]$ is the concentration of the $\beta$-anomer, $k_{M1}$ is the rate constant for conversion from $\alpha$-glucoside to $\beta$-glucoside, and $k_{M-1}$ is that in the opposite direction (defined in Scheme 1). The differential equation for the rate of change in $\alpha$-anomer concentration is similar. Integration of these differential equations gives[37]

$$[\alpha(t)] = \frac{[A]_0(k_{M1}e^{-(k_{M1}+k_{M-1})t} + k_{M-1})}{(k_{M1} + k_{M-1})} \tag{2}$$

$$[\beta(t)] = \frac{[A]_0(k_{M1} - k_{M1}e^{-(k_{M1}+k_{M-1})t})}{(k_{M1} + k_{M-1})} \tag{3}$$

The rate constants that characterize mutarotation were estimated by fitting the functions to experimental time courses according to the scheme of opposing unimolecular reactions, using the special case of a system that initially contains only one form of reactant ($[A]_0$ in eqs 2 and 3).

The digestion kinetics were determined by measuring the initial velocities of glucose and oligoglucoside production. Parabolas were fitted to the initial stages of glucose/glucoside concentration curves and the slope (derivative) was determined at $t = 0$ and at the commencement of the SDS stage. The substrate concentrations used for estimating the value of the Michaelis constant, that applied at the start of the SDS stage of the reaction, were obtained by subtracting the measured amount of starch digested (inferred from the amount of free glucose estimated from the NMR spectra) from the initial amount of starch. These data were then analyzed using Lineweaver−Burk plots to estimate the value of the Michaelis−Menten constant, $K_m$, and the maximum velocity, $V_{max}$. All equations were fitted using the NonlinearRegression function in *Mathematica* 6.0 (Wolfram, Champaign, IL).

## Results and Discussion

**Mutarotation of Glucose.** To validate our NMR method the mutarotation kinetic of $\alpha$-D-glucose was measured. There are two anomeric forms of all glucose-containing products of digestion that were important in the present study. The two ring structures of glucose are the $\alpha$- and $\beta$-anomers (Figure 1). These differ structurally by the relative position of their hydroxyl on C-1 of the pyranose ring. The $\alpha$- and $\beta$-forms of glucose and oligoglucosides interconvert in an acid/base-catalyzed reaction with a lifetime of minutes to hours, in aqueous solutions. The equilibrium ratio for glucose at pH 7.0 is $\alpha/\beta = 36{:}64$ at 25 °C.[36] The ^{1}H NMR resonances of the anomeric protons at the reducing end of oligoglucosides, including those of free glucose, are at 5.2 ppm for $\alpha$- and 4.6 ppm for $\beta$-anomers, respectively, so the anomers are readily resolved under most experimental conditions.[38]

Eqs 2 and 3 were fitted to the time course data. Values of $k_{M1} = (1.49 \pm 0.04) \times 10^{-4}$ s$^{-1}$ and $k_{M-1} = (2.64 \pm 0.08) \times 10^{-4}$ s$^{-1}$ were estimated for aqueous samples at pH 7.0 and 25 °C (Figure 2). Previous work[36] involved measuring these kinetic constants by polarimetry with the values under the same
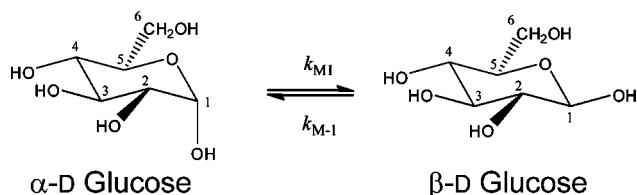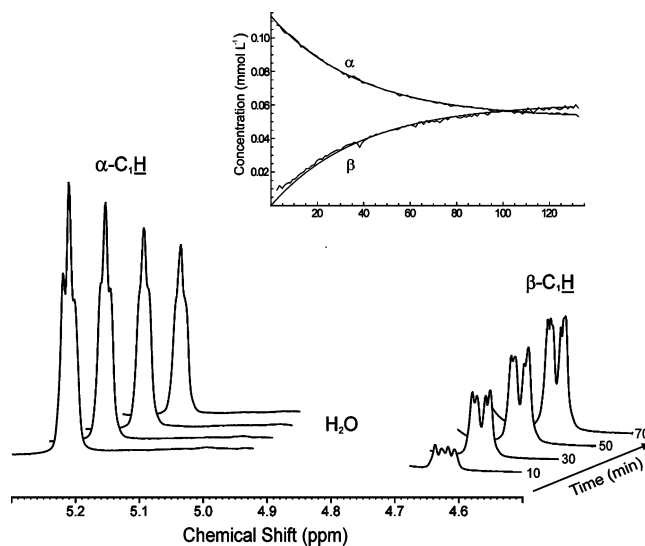


**Figure 2.** Time evolution of ^{1}H NMR (400.13 MHz) spectra showing the mutarotation of $\alpha$-glucose to $\beta$-glucose, at 25 °C and pH 5.3. Inset: Progress curves showing the experimental data and fit of the conversion of the $\alpha$-anomer into the $\beta$-anomer.

conditions being $k_{M1} = 1.44 \times 10^{-4}$ s$^{-1}$ and $k_{M-1} = 2.55 \times 10^{-4}$ s$^{-1}$. Our values are in excellent agreement with these, giving credence to the present NMR procedure for kinetic applications.

As the rate of mutarotation is known to be dependent on conditions such as the pH, it was also important to measure it at pH 5.3, and 25 °C, and in the presence of starch, as these were the conditions under which the digestions were studied. The results showed slightly larger values of the rate constants ($k_{M1} = (1.59 \pm 0.05) \times 10^{-4}$ s$^{-1}$ and $k_{M-1} = (2.83 \pm 0.08) \times 10^{-4}$ s$^{-1}$), as expected for this acid/base-catalyzed reaction.

Considering the multiple-step process of digestion (Scheme 1), the Michaelis−Menten parameters were found by measuring the initial velocity of the sum of both the normalized $\alpha$- and $\beta$-integrals, allowing the kinetics of mutarotation to be disregarded. However, it was also possible to check the validity of the entire scheme by fitting each anomer's data separately using all the already estimated constants but floating the time taken for the RDS stage to complete (data not shown). And we note that using NMR spectroscopy to monitor digestion reactions has advantages over other methods because of its ability to separately detect the different anomeric products; in addition, NMR spectroscopy is able to measure the concentration of oligosaccharides that are produced during a digestion with $\alpha$-amylase. This is done without further digestion with an exohydrolase, that is traditionally used to completely digest all oligosaccharides to glucose for quantitative analysis.

Note that during the digestion reactions the enzymes, due to their specificity, created only one type of glucose or glucoside anomer.[39] It was obvious from the NMR spectra which anomer was produced by each enzyme, as initially only one set of anomer resonances appeared.

**Kinetics of Starch Digestion.** During the course of in vivo starch digestion, glucose and short-chain oligoglucosides are produced. To understand this process with its many parallel pathways, two enzymes, which play a major role in the digestion of starch in the body, were studied separately in vitro (Scheme 1). The Michaelis−Menten differential equation (eq 4) describes the kinetics of many regular enzymatic processes



**Figure 1.** Mutarotation of glucose. The rate constants that characterize the forward and reverse reactions are denoted by $k_{M1}$ and $k_{M-1}$. The equilibrium position of the reaction is similar for all hexoses.

$$\frac{d[P]}{dt} = \frac{V_{max}[S]}{K_m + [S]} \qquad (4)$$

where numerical integration of the differential equation describes time course data for given values of the Michaelis constant, $K_m = (k_{-1} + k_2)/k_1$ ($k_1$, $k_{-1}$, $k_2$ are defined in Scheme 1), and the maximum velocity, $V_{max} = [E_0]k_2$ (where $[P]$, $[S]$ and $[E_0]$ are concentrations of product, substrate, and enzyme initially, respectively). It is well-known that there are two or more stages (rapidly digested starch, RDS, and slowly digested starch, SDS) during starch digestion by hydrolases.[19,32,33] However, kinetic models that are currently used to fit starch digestion curves disregard the deviation from normal Michaelis–Menten kinetics. Hence, an approach that uses a simple kinetic model during each distinct stage was advocated. Data from each of two apparent steps in the digestion time courses were analyzed graphically using Lineweaver–Burk plots.

$$\frac{1}{V} = \frac{K_m}{V_{max}[S]} + \frac{1}{V_{max}} \qquad (5)$$

This approach was necessary as the digestion data were not able to be fitted by a simple Michaelis–Menten equation although the initial velocities of the reaction were readily measured for each of two stages for a range of substrate concentrations.

The reaction of α-amylase with starch yields short chain α-oligoglucosides, generally no longer than four glucose residues.[40] This reaction is mechanistically similar for amyloglucosidase, although the enzyme releases exclusively single glucose molecules. Also, amyloglucosidase solely produced the β-anomer of glucose, which then underwent mutarotation to yield the α-anomer.

During hydrolysis with α-amylase (Figure 3), three spectral lines were well resolved and were useful for monitoring the progress of the reaction: (1) Before the enzyme was added, the small resonance assigned to the H atom on the $C_1$ of α-(1,4) linked glucosyl was present at 5.4 ppm, along with those of α- and β-anomers from the reducing ends of the glucose residues in the starch (5.2 and 4.6 ppm, respectively). The well-resolved resonances suggested that the atoms were mobile and, hence, the residues were solubilized in solution; (2) as the digestion proceeded with α-amylase, the intensity of the resonance from the α-(1,4) linkage-$C_1\underline{H}$ increased (Figure 3). Oligoglucoside products have α-(1,4)-linkages so the signal grew as starch was hydrolyzed although deviated from typical Michaelis–Menten kinetics prior to hydrolysis of SDS. Much later, the resonance intensity finally reached a limiting value, indicating completion

of the reaction (not shown in Figures 3 or 4). The α-(1,4) reducing end signal of the oligosaccharide reached a plateau after the RDS stage as the kinetics of oligosaccharide production by α-amylase reached a similar rate, during the SDS stage, to the depletion of the α-anomer by mutarotation. This plateau was also an obvious sign of the change of stages in the rate of the enzyme kinetic.

In the case of amyloglucosidase (Figure 4), the $^1$H NMR resonance from α-(1,4) linkage-$C_1\underline{H}$ decreased rapidly as the digestion proceeded; in this process single glucose molecules are released. As there was no residual α-(1,4) linkage-$C_1\underline{H}$ resonance at times after glucose release had slowed (after the RDS stage), we inferred that the remaining substrate was insoluble in water, as only soluble solutes give visible resonances in conventional solution-state NMR spectra.[13] It was concluded that the lower rate of glucose release was due to the diminution of starch in aqueous solution. (3) As the concentration of digestible starch was reduced to zero by α-amylase, the signal of the α-(1,4) linkage-$C_1\underline{H}$ appeared exclusively due to oligosaccharide product (Figure 5) and not the insoluble starch substrate. Therefore, the normalized resonance intensity of α-(1,4) linkage-$C_1\underline{H}$ relative to the resonance intensity from the reducing ends of oligosaccharide, approached a plateau. Therefore, from the normalized α-(1,4) linkage-$C_1\underline{H}$ signal and total signal from the reducing end of oligosaccharides, the number-average length of oligosaccharides was calculated. It fell between 3 and 3.5 for α-amylase and was always 1 for amyloglucosidase, independent of the nature of the initial substrate or experimental conditions.

**Time Courses.** From the time dependence of the emergence of the $-C_1\underline{H}$ resonance of each glucose anomer (Figure 5), it was possible to deduce which anomer of mono- or oligoglucosides was released from the starch. There was also an obvious transition in the velocity of the reaction from a high value to a much lower one after the initial stages of each time course. Thus, there were (at least) two fractions of starch being digested. The time courses showed deviation from what was predicted for a simple Michaelis–Menten enzyme, so it was postulated that the deviation was due to a change in the substrate and how it interacts with the enzyme. Thus each time course was analyzed as if it had two stages. Michaelis–Menten parameters were estimated for both the rapid phase and the slow phase of the reaction by using estimates of initial velocities from each. The data were fitted using the following approach: (1) the velocity was measured from the initial slope of a parabola that was fitted to the total amount of glucose or oligosaccharide produced during each stage in the time course; (2) the total concentration
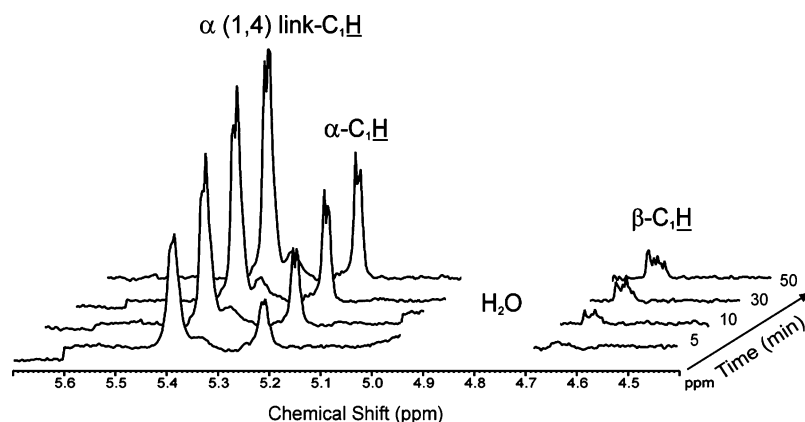


**Figure 3.** $^1$H NMR (400.13 MHz) spectra showing the time dependence of digestion of starch (4% w/w) by α-amylase (3 U mL$^{-1}$). Temperature was 25 °C, acetate buffer pH 5.3. Note: The signal at 5.4 ppm arose from the proton resonance on $C_1$ of an α-(1,4) linkage.
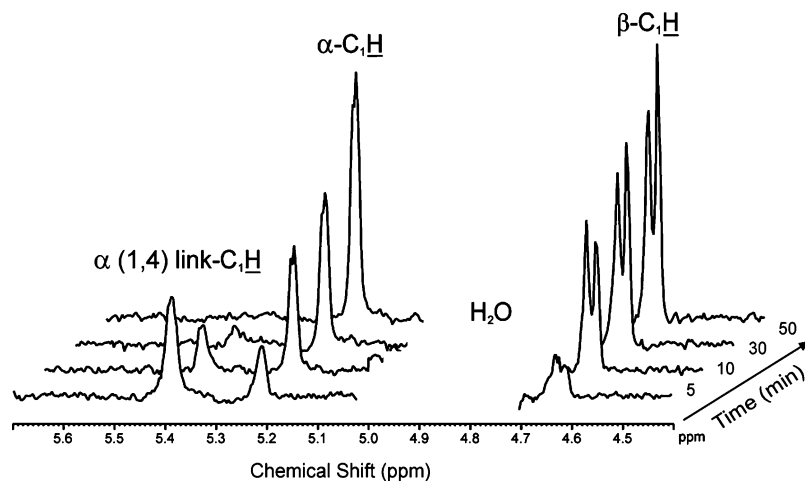
**Figure 4.** ^{1}H NMR (400.13 MHz) spectra showing the time dependence of digestion of starch (4% w/w) by amyloglucosidase (0.3 U mL$^{-1}$). Temperature was 25 °C, acetate buffer pH 5.3. Note: The signal at 5.4 ppm arose from the proton resonance on C$_1$ of an α-(1,4) linkage.
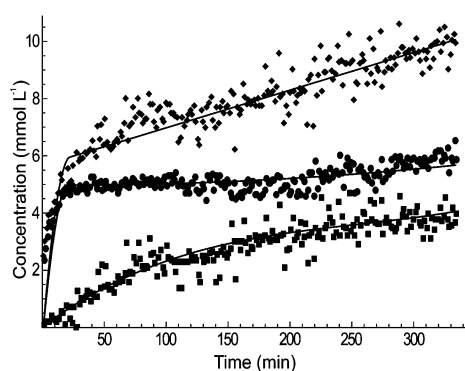


**Figure 5.** Time dependence of the concentration of the each oligosaccharide anomer from starch (Sigma) by the action of α-amylase at 25 °C. The α-anomers (circles) were generated by hydrolysis and then converted to the β-anomers (squares) via mutarotation. Summing the concentrations of α- and β-anomers gave the total concentration of glucose/oligoglucoside reducing end units (diamonds). The empirical, fitted solid lines were drawn to highlight the deviation observed from regular enzyme kinetics (for product, P, concentrations, the fitted lines were: total glucose concentration (top curve) $[P] = -0.00333t^2 + 0.4t$, where $t$ denotes time, for $t < 20$ min and $[P] = 0.0121t + 5.75$ for $t \geq 20$ min; for the α-anomer alone (middle curve) $[P] = -0.00236t^2 + 0.283t$ for $t < 20$ min and $[P] = 0.00214t + 4.6$ for $t \geq 20$ min; for the β-anomer alone (bottom curve) $[P] = -0.000016t^2 + 0.016t$).



**Figure 6.** Data taken from Apar and Ozbek[33] of 8, 4, 2, and 1 (g dL$^{-1}$) starch solution (corresponding to Figure 1 in the original paper). The exponential function used by the authors for fitting (dashed line) their data and the multiple stage fits (unbroken line) used to generate Lineweaver−Burk plots. Inset: The Lineweaver−Burk plot of the RDS (open circles) and SDS (closed circles) stages for the range of starch concentrations in each stage of the starch digestion.[33]

of starch was used in the Lineweaver−Burk plot for each stage, not the amount of dissolved or undigested starch.

We also applied the fitting procedure to previously reported data.[33] This is the only large data set to have reported on the two stages, rapidly digested starch (RDS) and slowly digested starch (SDS). Figure 6 shows the two curves that were fitted to the data to estimate the initial velocities. The new analysis gave a better description of the results than the exponential function that was used previously.[33] Furthermore, the initial velocities recorded as a function of starch concentration gave linear Lineweaver−Burk plots (Figure 6 inset) indicating consistency with simple Michaelis−Menten kinetics.

**Lineweaver−Burk Plots.** Both enzymes tested (α-amylase and amyloglucosidase) showed clear stages during digestion of different samples, suggesting that a change in the nature of the starch rather than a characteristic of the enzymes determines the rate of digestion (Figure 7). (NB: There was no evidence of product inhibition by glucose or oligosaccharides at the concentration produced during digestion,[34,41] data not shown.) For
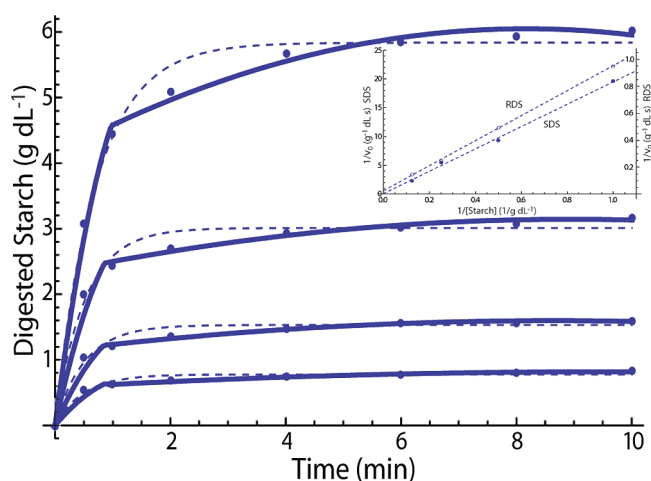
both enzymes and types of starch, the maximum velocity was decreased from RDS to SDS, although no significant difference in these values was found between starch samples (Table 2). The observation that there was no significant difference in $V_{max}$ in wheat flour and an extracted starch sample implied that protein and lipid binding to starch did not significantly affect the rate of digestion. The substrate concentration that gives half the maximum velocity is the $K_m$, and this varied with each of the two stages of digestion with amyloglucosidase and with the type of enzyme (Table 3). Significant differences in $K_m$ were also noted for the two types of starch for α-amylase, but not for the RDS and SDS stages. Amyloglucosidase acted differently having significant differences in $K_m$ between the two stages of digestion and not with the different starch samples.

Spectrophotometric assays of glucose concentration have been used to monitor starch digestion in vitro, and the distinct stages or phases of the time courses have been reported.[19,42] Although a multistage process has been observed for starch digestion, kinetic models used to describe each stage in the progress of the reactions had not been used. Instead variations have been made in a single Michaelis−Menten expression to yield
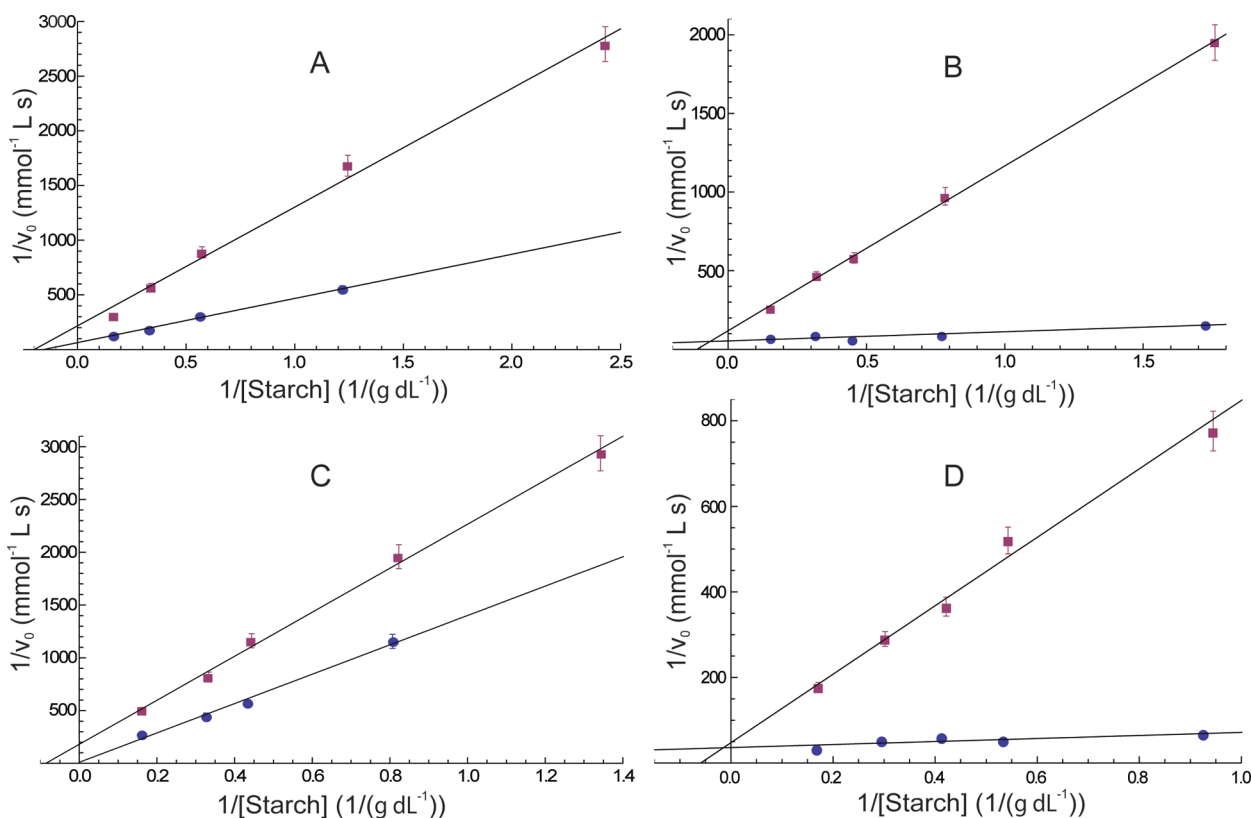
**Figure 7.** Lineweaver–Burk plots for the initial stage (circles) and the second stage (squares) of the digestion of (a) 0.5 $\mu$L (1.5 U) of $\alpha$-amylase in 0.5 mL of starch (Sigma) reaction mixture; (b) 0.5 $\mu$L (0.15 U) of amyloglucosidase in 0.5 mL of starch (Sigma) reaction mixture; (c) 5 $\mu$L (15 U) of $\alpha$-amylase in 0.5 mL of wheat flour reaction mixture; and (d) 5 $\mu$L (1.5 U) of amyloglucosidase in 0.5 mL of wheat flour reaction mixture.

**Table 2.** Maximum Reaction Velocity $V_{max}$ (mmol L$^{-1}$ s$^{-1}$)

| | $\alpha$-amylase | | amyloglucosidase | |
|---|---|---|---|---|
| substrate | 1st stage | 2nd stage | 1st stage | 2nd stage |
| starch | 0.016 ± 0.002[a] | 0.005 ± 0.001 | 0.019 ± 0.004 | 0.009 ± 0.001 |
| wheat flour | 0.017 ± 0.009 | 0.006 ± 0.002 | 0.028 ± 0.006 | 0.018 ± 0.009 |

[a] Denotes ± standard deviation.

**Table 3.** Michaelis-Menten Constant $K_m$ (g dL$^{-1}$ (% w/v))

| | $\alpha$-amylase | | amyloglucosidase | |
|---|---|---|---|---|
| substrate | 1st stage | 2nd stage | 1st stage | 2nd stage |
| starch | 6.4 ± 0.8[a] | 5.1 ± 1.5 | 1.1 ± 0.3 | 9.1 ± 1.0 |
| wheat flour | 22.0 ± 11.6 | 11.8 ± 3.1 | 1.0 ± 0.4 | 14.5 ± 10.0 |

[a] Denotes ± standard deviation.

consistent estimates of $V_{max}$ and $K_m$ for the different starch samples.[22,30,43] Previous models warrant refinement, as an unnecessarily large number of parameters are used for regression analysis; while the new approach of mathematically acknowledging the existence of two (or more) stages of starch hydrolysis provides a physically rational basis for the interpretation of the kinetics. In the present study, Michaelis–Menten kinetics was assumed to describe each of the two stages thus minimizing the number of fitting parameters.

## Conclusions

Time-resolved $^1$H NMR spectroscopy, using the CPMG pulse sequence, was shown to be valuable for monitoring the kinetics of starch digestion in vitro by an endo- and an exohydrolase. The approach was applied to crude flour and purified starch and is potentially applicable to many forms of starch; these include extracted starch, milled flour, and cooked-, uncooked-, macerated-, and whole-grain starch. The methodology for recording the progress of the reaction is less time-consuming than current assays that rely on chemical analysis of glucose,[22,28,29] and it yields large data sets including, for the first time, the initial phase of hydrolysis, typically in the first 5% of the extent of reaction. It is this early stage of starch digestion that determines the initial rate of absorption of sugar into the blood stream. The kinetic analysis implies that protein and lipid binding to starch does not significantly decrease the rate of digestion at concentrations where the substrate saturates the enzyme(s).

Although we are aware of the many different chemical and physical properties affecting the digestion parameters of carbohydrates the purpose of the present study was not to correlate these properties with the functional property of digestion. Alternately, a new methodology to monitor starch digestion and present a different approach to kinetically analyzing the digestion of carbohydrate was presented. Experimental data from previous work[33] was also able to be fitted with better precision, and a lower number of parameters were required to describe the experimental data. The method developed should be important for the rational design of diets as it should enable digestion characteristics of rapidly and slowly digested starch to be quantified in complex mixtures of food.

## References and Notes

(1) Bednar, G. E.; Patil, A. R.; Murray, S. M.; Grieshop, C. M.; Merchen, N. R.; Fahey, G. C. *J. Nutr.* **2001**, *131*, 276–286.

(2) Tharanathan, R. N.; Mahadevamma, S. *Trends Food Sci. Technol.* **2003**, *14*, 507–518.

(3) Conde-Petit, B.; Nuessli, J.; Arrigoni, E.; Escher, F.; Amado, R. *Chimia* **2001**, *55*, 201–205.

(4) Buleon, A.; Colonna, P.; Planchot, V.; Ball, S. *Int. J. Biol. Macromol.* **1998**, *23*, 85–112.

(5) Ball, S.; Guan, H. P.; James, M.; Myers, A.; Keeling, P.; Mouille, G.; Buleon, A.; Colonna, P.; Preiss, J. *Cell* **1996**, *86*, 349–352.

(6) Bello-Perez, L. A.; Paredes-Lopez, O.; Roger, P.; Colonna, P. *Food Chem.* **1996**, *56*, 171–176.

(7) Farhat, I. A. In *Modern Magnetic Resonance*; Webb, G. A., Ed.; Springer-Verlag: Hamburg, 2006; Part 3, pp 1877−1885.

(8) Tang, H.; Wang, Y. In *Modern Magnetic Resonance*; Webb, G. A., Ed.; Springer-Verlag: Hamburg, 2006; Part 3, pp 1723−1732.

(9) Coen, M.; Bodkin, J.; Power, D.; Bubb, W. A.; Himmelreich, U.; Kuchel, P. W.; Sorrell, T. C. *Antimicrob. Agents Chemother.* **2006**, *50*, 4018–4026.

(10) Plummer, R.; Bodkin, J.; Yau, T. W.; Power, D.; Pantarat, N.; Larkin, T. J.; Szekely, D.; Bubb, W. A.; Sorrell, T. C.; Kuchel, P. W. *Magn. Reson. Med.* **2007**, *58*, 656–665.

(11) Torres, A. M.; Bansal, P. S.; Alewood, P. F.; Geraghty, D. P.; Kuchel, P. W. *D Amino Acids* **2007**, 379−387.

(12) De Bruyn, H.; Sprong, E.; Gaborieau, M.; David, G.; Roper, J. A.; Gilbert, R. G. *J. Polym. Sci., Part A: Polym. Chem.* **2006**, *44*, 5832–5845.

(13) Dona, A.; Yuen, C.-W. W.; Peate, J.; Gilbert, R. G.; Castignolles, P.; Gaborieau, M. *Carbohydr. Res.* **2007**, *342*, 2604–2610.

(14) Hernandez, J. M.; Gaborieau, M.; Castignolles, P.; Gidley, M. J.; Myers, A. M.; Gilbert, R. G. *Biomacromolecules* **2008**, *9*, 954–965.

(15) Mange, S.; Dever, C.; DeBruyn, H.; Gaborieau, M.; Castignolles, P.; Gilbert, R. G. *Biomacromolecules* **2007**, *8*, 1816–1823.

(16) Krezowski, P. A.; Nuttall, F. Q.; Gannon, M. C.; Bartosh, N. H. *Am. J. Clin. Nutr.* **1986**, *44*, 847–856.

(17) Thorne, M. J.; Thompson, L. U.; Jenkins, D. J. A. *Am. J. Clin. Nutr.* **1983**, *38*, 481–488.

(18) Brand-Miller, J. C.; Holt, S. H. A.; Pawlak, D. B.; McMillan, J. *Am. J. Clin. Nutr.* **2002**, *76*, 281S–285S.

(19) Englyst, H. N.; Kingman, S. M.; Cummings, J. H. *Eur. J. Clin. Nutr.* **1992**, *46*, S33−50, Suppl 2.

(20) Duggleby, R. G. *Meth. Enzymol.* **2001**, *24*, 168–174.

(21) Zhang, G.; Ao, Z.; Hamaker, B. R. *Biomacromolecules* **2006**, *7*, 3252–3258.

(22) Goni, I.; Garcia-Alonso, A.; Saura-Calixto, F. *Nutr. Res. (N.Y.)* **1997**, *17*, 427–437.

(23) Okuda, M.; Aramaki, I.; Koseki, T.; Satoh, H.; Hashizume, K. *Cereal Chem.* **2005**, *82*, 361–368.

(24) DeVries, J. W. *Cereal Foods World* **2007**, *52*, 45–49.

(25) Jenkins, D. J.; Wolever, T. M.; Taylor, R. H.; Barker, H.; Fielden, H.; Baldwin, J. M.; Bowling, A. C.; Newman, H. C.; Jenkins, A. L.; Goff, D. V. *Am. J. Clin. Nutr.* **1981**, *34*, 362–366.

(26) Roberts, S. B. *Nutr. Rev.* **2000**, *58*, 163–169.

(27) Jenkins, D. J.A.; Kendall, C. W. C.; Augustin, L. S. A.; Franceschi, S.; Hamidi, M.; Marchie, A.; Jenkins, A. L.; Axelsen, M. *Am. J. Clin. Nutr.* **2002**, *76*, 266S–273S.

(28) Sayago-Ayerdi, S. G.; Tovar, J.; Osorio-Diaz, P.; Paredes-Lopez, O.; Bello-Perez, L. A. *J. Agric. Food Chem.* **2005**, *53*, 1281–1285.

(29) Shu, X.; Jiao, G.; Fitzgerald, M. A.; Yang, C.; Shu, Q.; Wu, D. *Starch/Staerke* **2006**, *58*, 411–417.

(30) Amato, M. E.; Ansanelli, G.; Fisichella, S.; Lamanna, R.; Scarlata, G.; Sobolev, A. P.; Segre, A. *J. Agric. Food Chem.* **2004**, *52*, 823–831.

(31) Akerberg, C.; Zacchi, G.; Torto, N.; Gorton, L. *J. Chem. Technol. Biotechnol.* **2000**, *75*, 306–314.

(32) Ao, Z.; Simsek, S.; Zhang, G.; Venkatachalam, M.; Reuhs, B. L.; Hamaker, B. R. *J. Agric. Food Chem.* **2007**, *55*, 4540–4547.

(33) Apar, D. K.; Ozbek, B. *Chem. Eng. Commun.* **2007**, *194*, 334–344.

(34) Wang, J.-P.; Zeng, A.-W.; Liu, Z.; Yuan, X.-G. *J. Chem. Technol. Biotechnol.* **2006**, *81*, 727–729.

(35) Meiboom, S.; Gill, D. *Rev. Sci. Instrum.* **1958**, *29*, 688–691.

(36) Kendrew, J. C.; Moelwyn-Hughes, E. A. *Proc. R. Soc. (London)* **1940**, *A176*, 352–367.

(37) Mulquiney, P. J.; Kuchel, P. W. *Modelling Metabolism with Mathematica*; CRC Press: Boca Raton, FL, 2003; p 328.

(38) McIntyre, D. D.; Ho, C.; Vogel, H. J. *Starch/Staerke* **1990**, *42*, 260–267.

(39) Chiba, S.; Kimura, A.; Matsui, H. *Agric. Biol. Chem.* **1983**, *47*, 1741–1746.

(40) Kennedy, J. F. *Starch/Staerke* **1977**, *29*, 114–117.

(41) Lim, S.-T.; Lee, J.-H.; Shin, D.-H.; Lim, H. S. *Starch/Staerke* **1999**, *51*, 120–125.

(42) Chung, H.-J.; Yoo, B.; Lim, S.-T. *Starch/Staerke* **2005**, *57*, 354–362.

(43) Komolprasert, V.; Ofoli, R. Y. *J. Chem. Technol. Biotechnol.* **1991**, *51*, 209–223.